HHS Public Access

Author manuscript

J Immunol. Author manuscript; available in PMC 2016 October 01.

Published in final edited form as:

J Immunol. 2015 October 1; 195(7): 3227–3236. doi:10.4049/jimmunol.1402699.

Regulatory and Helper Follicular T cells and antibody avidity to SIV-gp120

Matthew J. Blackburn[*], **Ma Zhong-Min**[†], **Francesca Caccuri**[*], **Katherine McKinnon**[*], **Luca Schifanella**[*], **Yongjun Guan**[‡], **Giacomo Gorini**[*], **David Venzon**[§], **Claudio Fenizia**[*], **Nicolò Binello**[*], **Shari N. Gordon**[*], **Christopher J. Miller**[†], **Genoveffa Franchini**[*], and **Monica Vaccari**[*,¶]

[*]Animal Models and Retroviral Vaccine Section, National Cancer Institute, Bethesda, Maryland, USA

[†]California National Primate Research Center, University of California Davis, Davis, California, USA

[‡]Department of Microbial Pathogenesis, University of Maryland School of Dentistry, Baltimore, Maryland, USA

[§]Biostatistics and Data Management Section, National Cancer Institute, National Institutes of Health, Bethesda, Maryland, USA

Abstract

T follicular regulatory cells (T_{FR}) are a suppressive $CD4^+$ T cell subset that migrates to germinal centers (GC) during antigen presentation by up-regulating the chemokine receptor CXCR5. In the GC, T_{FR} control T follicular helper cells (T_{FH}) expansion and modulate the development of high-affinity antigen specific responses. Here we identified and characterized T_{FR} as $CXCR5^+$ $CCR7^-$-"follicular" T regulatory cells (T_{REG}) in lymphoid tissues of healthy rhesus macaques, and we studied their dynamic throughout infection in a well-defined animal model of HIV pathogenesis. T_{FR} were infected by SIV_{mac251} and had comparable levels of SIV-DNA to $CXCR5^-$ $CCR7^+$-"T-zone" T_{REG} and T_{FH}. Contrary to the SIV-associated T_{FH} expansion in the chronic phase of infection, we observed an apparent reduction of T_{FR} frequency in cell suspension, as well as a decrease of $CD3^+$ $Foxp3^+$ cells in the GC of intact lymph nodes. T_{FR} frequency was inversely associated with the percentage of T_{FH} and, interestingly, with the avidity of the antibodies that recognize the SIV-gp120 envelope protein. Our findings show changes in the T_{FH}/T_{FR} ratio during chronic infection and suggest possible mechanisms for the unchecked expansion of T_{FH} cells in HIV/SIV infection.

[¶]Corresponding author: Address correspondence to Monica Vaccari, Phone: (301)-402-0442; Fax: (301)-402-0055; Address: 9000 Rockville Pike, Building 41 Room C303, Bethesda, MD 20892; vaccarim@mail.nih.gov.
Francesca Caccuri's current address: Department of Molecular and Translational Medicine, University of Brescia, Brescia, Italy.

Disclosures

The authors have no financial conflicts of interest.

Introduction

The generation of long-lived plasma cells and high affinity antibodies is largely dependent on T-B-cell interaction in the B-follicles of secondary lymphoid organs (1) (2) (3). Antigen-activated B cells making contact with a specialized subset of $CD4^+$ T cells, called T follicular helper cells (T_{FH}), can enter the germinal centers (GCs) to undergo to somatic hypermutation and affinity maturation (4). T_{FH} home to B follicles and GC (5) (6, 7) (8, 9) by up-regulating the chemokine (C-X-C motif) receptor 5 (CXCR5) and down-regulating the chemokine (C-C motif) receptor 7 (CCR7) (10)(5)(6). T_{FH} express high levels of programmed death 1 (PD-1), inducible co-stimulator (ICOS), and Bcl-6, a master transcriptional regulator that orchestrates T_{FH} differentiation (11)(12)(13). In the GC, T_{FH} provide signals for B-cell survival and differentiation (10)(5) via IL-21 production and CD40L expression, and they promote the generation of antibodies with high affinity (11)(12)(13, 14)(15)(16).

GC reactions are tightly regulated to prevent the emergence of B-cell clones that are specific or cross-reactive against self-antigens, while selecting for high affinity antibodies to microbes (17)(18). The maintenance of the appropriate number of T_{FH} is crucial (19); the absence of T_{FH} has a negative impact in the generation of the GC (20)(21), while their excessive accumulation leads to increased GC reactions and the onset of some autoimmune diseases (4)(22)(23)(24).

$CD4^+$ T follicular regulatory cells (T_{FR}) contain T_{FH} numbers and in doing so, they control the magnitude of GC responses (25) (26). Similarly to T_{FH}, T_{FR} migrate to the GC by expressing CXCR5 and down regulating CCR7 during T-cell activation (6)(27)(28)(29)(25). T_{FR} differentiate from natural $CXCR5^-$ $Foxp3^+$ $CD25^+$-T_{REG} and express high levels of the typical T_{REG} markers (i.e. Foxp3, CD25, CTLA-4) and T_{FH} canonical markers such as ICOS, PD-1 and Bcl-6 (25) (26). While Bcl-6 is essential for CXCR5 expression on B- and T_{FH} cells and for their localization to the GC (25)(26), T_{FR} co-express Blimp-1, which is known to repress CXCR5 expression (25)(30). Ablation of the activated T-cell nuclear factor (NFAT)-2 in mice results in reduced expression of CXCR5 on T_{FR}, but not on T_{FH}, suggesting that this transcriptional factor may enable the proper localization of T_{FR} within B-cell follicles, possibly by inhibiting Blimp-1–mediated repression of CXCR5 expression (31). T_{FR} restrict T_{FH} numbers, and help to maintain a steady ratio of IgM^+ to IgM^- (switched) B cells (32) via IL-10 production (29); *in vivo* depletion of $CD4^+$ T cells with suppressive activity including T_{FR}, or *in vivo* blockade of IL-10 or transforming grow factor –β (TGF-β) receptors results in T_{FH} expansion, loss of normal proportion of IgM^- B cells and in increased levels of high affinity antibodies (26) (29)(33).

A hallmark of HIV and SIV infection is the immune dysfunction of humoral responses characterized by loss of memory B cells and hypergammaglobulinemia (34) (35). T_{FH} frequency is significantly increased in the lymph nodes of HIV infected individuals and chronically SIV_{mac251} infected macaques (8)(36). Production of the IL-21 cytokine by T_{FH} is significantly reduced during HIV/SIV infection, possibly affecting GC homeostasis and the development of effective humoral responses to the virus (37). The HIV/SIV associated changes in T_{FH} number and function may contribute to the impairment of B-cell responses

(9)(36)(38), however other studies have found associations between the levels of functional T_{FH} and broadly neutralizing antibodies in chronic HIV patients (39). While the relative role of T_{FH} in HIV pathogenesis needs further investigation, it would be important to understand the molecular and cellular mechanisms that regulate T_{FH} expansion.

T_{FR} dynamic in HIV-infection has not been investigated yet. We identified T_{FR} as $CXCR5^+$-T_{REG} in the lymph nodes of rhesus macaques, a well-established model of HIV infection. We show that 1) T_{FR} are infected by SIV_{mac251}, 2) there is an apparent decrease in T_{FR} levels, particularly during chronic infection, 3) T_{FR} levels are associated with the levels of T_{FH} and the total frequency of IgG^+ B cells, and 4) T_{FR} levels are inversely correlated with the avidity of antibodies to SIV-gp120 protein. Taken together these findings suggest a potential role for T_{FR} in modulating humoral responses against HIV/SIV.

Materials and Methods

Animals and challenge

All of the animals used in this study were colony-bred rhesus macaques (Macaca mulatta) obtained from Covance Research Products (Alice, TX). The animals were housed and maintained in accordance with the standards of the Association for the Assessment and Accreditation of Laboratory Animal Care (AAALAC). This study was carried out in strict accordance with the recommendations in the Guide for the Care and Use of Laboratory Animals of the National Institutes of Health. All surgery was performed under general anesthesia, and all efforts were made to minimize suffering. All macaques were negative for simian retrovirus, simian T-cell leukemia virus type 1, and herpesvirus B. Macaques were infected with a single high dose (6300 $TCID_{50}$) (40) or with 10 repeated low doses (120 $TCID_{50}$) of SIV_{mac251} given rectally (41) (Table I).

Cell isolation from lymph nodes and mucosa

Cells were isolated from blood, lymph nodes and spleen by density-gradient centrifugation. Tissues from the rectum, jejunum and colon were treated with 1 mM Ultra Pure DTT (Invitrogen Life Technologies) for 30 min followed by incubation in calcium/magnesium-free HBSS (Invitrogen Life Technologies) for 60 min with stirring at room temperature to remove the epithelial layer. Lamina propria lymphocytes were separated by cutting the tissue into small pieces and incubating in 10% FBS IMDM (Invitrogen Life Technologies) with collagenase D (400 U/ml; Boehringer Mannheim) and DNase (1 μg/ml; Invitrogen Life Technologies) for 2.5 h at 37°C. Mononuclear cells were placed over 42% Percoll (General Electric Healthcare) and centrifuged at 800 × *g* for 25 min at 4°C. Lamina propria lymphocytes were collected from the cell pellet (42).

Antibodies & staining

We used the following antibodies: CD3-Alexa700 (SP34-2), CD4-PerCP-Cy5.5 (L200), CD95-PeCy5 (DX2), CD197-PeCy7 (CCR7, clone 3D12), CD25-APCcy7 (M-A251), CD195-PE (CCR5, clone 3A9), CD14-Alexa700 (M5E2), CD16-Alexa700 (3G8), CD56-Alexa700 (B159), IgM-PerCP-Cy5.5 (G20-127), IgG-Qdot605 (G18-145), Ki67-PE (B56), CD21-PECy7 (B-ly4), all from BD Biosciences; Bcl-6-PE (IG191E/A8); CD278-PacBlue

(ICOS, clone C398.4A), CD25-PacBlue (BC96), PD-1-APC (EH12.2H7), CD39-BV421 (MOCP-21), CD39 (A1) from BioLegend; Foxp3-FITC (PCH101), CXCR5-PE-eFluor610 (MU5UBEE), CD20-Qdot650 (2H7) all from eBioscience; CD103-FITC (αE integrin, clone 2G5), CD19-PE-Cy5 (J3-119), CD127-PE (eBioRDR5) from Beckman Coulter. The α4β7 antibody (Act-1) was obtained through the NIH Nonhuman Primate Reagent Resource Program (AIDS Reagent Program, Division of AIDS, NIAID, NIH). Vivid-amine-reactive dye was used to discriminate live/dead cells (Invitrogen). IgA-Texas Red (polyclonal) was obtained from SouthernBiotech, and CD38-FITC (clone AT-1) from StemCell.

For phenotypic characterization of $CD4^+$ T cells subsets, cells were stained with surface markers CD3, CD4, CD95, CD25, CCR7, CXCR5, ICOS and Vivid. Cells were then fixed and permeabilized according to eBioscience's instructions and stained with anti-Foxp3 and anti-Bcl-6 for 30 min. The appropriate isotype-matched control Ab was used to define positivity. T_{FR} cells were gated as live $CD3^+$ $CD4^+$ $CD95^+$ T cells, and their percentage was calculated as the frequency of $CXCR5^+$ & $CCR7^-$ within $Foxp3^+$ $CD25^+$ cells (% of T_{REG}) or within $CD95^+$ $CD4^+$ T cells (% of memory $CD4^+$ T cells) (26). Similarly, Double Positive were $CXCR5^+$ & $CCR7^+$ cells and $CCR7^+$-T_{REG} were $CXCR5^-$ & $CCR7^+$. Finally, T_{FH} cells were gated as $CXCR5^+$ $PD\text{-}1^{hi}$ cells within the Foxp3 negative region or the memory $CD4^+$ T cells population (Figure 1A).

B cells were gated as live/lineage negative (lin^{neg}: $CD3^-$ $CD14^-$ $CD16^-$ $CD56^-$) positive for CD20 and or CD19 markers. For plasmablasts, cells were stained with lineage markers, CD20, CD38, CD39, IgM, IgG and IgA. Cells were treated with Cytofix/Cytoperm (BD Biosciences) and stained with Ki67. Plasmablasts (PBs) were gated as lineage negative (lin^{neg} $CD20^+$ and/or $CD19^+$ $CD21^-$ $Ki67^+$ $CD38^+$ $CD39^+$ (43). Marker expression was analyzed with a LSRII flow cytometer using FACSDiva software (BD Biosciences). FACS analysis was performed using FlowJo software (Tree Star, Inc., Ashland, OR). A minimum of 10,000 cells per tube was analyzed.

$CD4^+$ T cells counts

The absolute number of $CD4^+$ T cells was calculated as previously described (44).

Sorting

To determine the RNA levels for IL-10, TGF-β and SIV-DNA, cells from lymph nodes were stained with Vivid, CD3, CD4, CD25, CCR7 and CXCR5. T_{FR} cells were defined as live $CD3^+$ $CD4^+$ $CD25^+$ $CXCR5^+$ & $CCR7^-$, T_{REGS} as $CXCR5^-$ & $CCR7^+$. For proliferation, $CD25^+$ $CD4^+$ T cells (live $CD3^+$ $CD4^+$ $CD25^+$) were sorted. Sorting was performed on a FACS ARIA (BD Biosciences).

Migration assay

Sorted live $CD3^+$ $CD4^+$ $CD25^+$ cells were migrated for 1 hour to 1μg/ml CXCL13 (R&D Systems, Cat no. 801-CX/CF) using 5μm Pore Polycarbonate Membrane inserts (Millipore).

Proliferation

Cell proliferation was determined by dilution of CFSE (Life Technologies). Briefly, CD25-depleted ($CD3^+$ $CD4^+$) cells were stained with CFSE for 10 minutes and were then placed in a 24-well plate in the presence or absence of CD3 (10 μg/ml; clone FN18) with soluble αCD28 (1 μg/ml; clone CD28.2), in the presence or absence of autologous $CD3^+$ $CD4^+$ $CD25^+$ cells migrated to CXCL13 (10:1 ratio), for 4 days. Cells were then stained and analyzed by FACS as described above.

Cyclosporin A in vitro treatment

Cells from lymph nodes were incubated 30h with 50ug of cyclosporine A (Sigma) and incubated for 6h with or without PMA and in the presence of brefeldin A (Golgi-Plug; BD Biosciences).

RT-PCR

Total RNA was extracted from whole tissue with RNeasy Plus (Qiagen) and reverse transcribed with the High-capacity cDNA reverse transcription kit (Applied Byosistems). After reverse transcription the relative amounts of transcripts were determined by real-time PCR with the SYBR Green qPCR Master Mix (Promega) using 0.2 μM of PCR primers for IL-10 (5′-AGAACCACGACCCAGACATC-3′ (forward), 5′-GGCCTTGCTCTTGTTTTCAC-3′ (reverse)), and transforming growth factor β (TGF-β). The TGF-β was described elsewhere (45). Quantification of cDNA was normalized in each reaction according to the internal β-actin control (5′-GGCACCCAGCACAATGAAG-3′ (forward), and 5′-GCTGATCCACATCTGCTGG-3′ (reverse)). A real-time nucleic acid sequence-based amplification (NASBA) assay was used to quantitative SIV-RNA in plasma (46). SIV-DNA was quantified as previously described (40).

Immunohistochemistry in lymph nodes

The primary antibodies included Anti-Foxp3 (Abcam, Rabbit), Anti-CD20 (DAKO, mouse Ig2a) and Anti-CD3 (UCD Rat). Tris-buffered saline with 0.05% Tween 20 was used for all washes. Antibody diluent (Dako, Inc., Carpinteria CA) was used for all antibody dilutions. For all primary antibodies, slides were subjected to an antigen retrieval step consisting of incubation in AR10 (Biogenex Inc, San Ramon, CA) for 2 min at 125 °C in the Digital Decloaking Chamber (Biocare Medical, Concord, CA) followed by cooling to 90 °C before rinsing in water. Primary antibodies were replaced by normal rabbit IgG, mouse IgG (Invitrogen, Grand Island, NY) and rat IgG (Vector, Burlingame, CA) were included with each staining series as the negative control. Nonspecific binding sites were blocked with 10% goat serum and 5% bovine serum albumin (BSA, Jackson ImmunoResearch, West Grove, PA). Binding of the primary antibodies was detected simultaneously using Alexafluor Goat anti Rat 568, Alex fluor Goat anti Mouse IgG2a 647, and Alex fluor Goat anti Rabbit 488. All slides were coverslipped using ProLong Gold with 4′, 6-diamidino-2-phenylindole dihydrochloride hydrate (DAPI, Molecular probes, Grand Island, NY) to stain nuclei. All the control experiments gave appropriate results with minimal nonspecific staining.

Slides were visualized with epi-fluorescent illumination using a Zeiss Axioplan 2 microscope (Carl Zeiss Inc., Thornwood, NY) and appropriate filters. Digital images were captured and analyzed by using Openlab software (Inprovision, Waltham, MA). Alex flour 647 was captured in black and white channel while other fluorescence dyes were pictured in color channels. Five high-power (40x) microscope fields were randomly chosen and captured digitally with the system described above. Each captured field includes an area of approximately 0.04 mm2. Only clearly positive cells with distinctly labeled nuclei (DAPI) and bright staining were considered positive. Individual positive cells in the five captured high-power microscope fields of the immunohistochemical stained tissue sections were counted manually by a single observer. The numbers of positive cells are presented as cells per square millimeter.

Avidity assay

Avidity was analyzed as previously described (41). Briefly, recombinant SIV gp120 protein made from codon-optimized SIV_{mac239} gp120 fused to the C-terminal tag of HIV-1 gp120 was used as an antigen for the capture ELISA to detect SIV Abs against conformational epitope. Antibody avidity was determined by parallel ELISA. Heat-inactivated plasma samples were serially diluted and applied to a 96-well plate capturing SIV_{mac239} gp120. After 1 h of incubation, the plate was washed and half the samples were treated with Tris-buffered saline (TBS), while the paired samples were treated with 1.5 M sodium thiocyanate (NaSCN; Sigma-Aldrich) for 10 min at room temperature. The plate was washed and a goat anti-monkey IgG-detecting Ab (Fitzgerald) was used. The avidity index (%) was calculated by taking the ratio of the NaSCN-treated plasma dilution giving an OD of 0.5 to the TBS-treated plasma dilution giving an OD of 0.5 and multiplying by 100. Plasma of uninfected normal macaques served as negative controls.

Statistical analysis

Tests of two groups of animals for differences between cell types, tissues or stages of infection were performed using the exact Wilcoxon rank sum test. Differences before and after infection within the same group of animals were assessed using the Wilcoxon signed rank test. Differences across three stages of infection were modeled using repeated measures analysis of variance when distributional assumptions were met. Correlation analyses were performed using the exact Spearman rank correlation method. Trends across three groups were assessed by the Jonckheere-Terpstra test. Due to the exploratory nature of this study, the p values reported were not corrected for multiple comparisons. Values of $p \leq 0.05$ were labeled statistically significant, and we note that for outcomes where all pairwise comparisons of three groups are possible, values of $p \leq 0.02$ remain significant after correction for the multiple tests.

Results

Characterization and tissue distribution of T_{FR} in naïve Rhesus macaques

T_{FR} localize in the GC of mice and humans (29)(25)(26)(47). We confirmed the presence of $Foxp3^+$ $CD3^+$ T cells in healthy macaque's B-cell follicles of lymph nodes, by immunohistochemistry (Figure 1A). We then characterized T_{FR} in cell suspension by flow

cytometry, and compared their frequency, phenotype and localization to that of $CCR7^+$-T_{REG} and T_{FH} cells. The gating strategy used to define these 3 cell subsets is shown in Figure 1B. T_{FR} and T_{REG} were gated within the live $Foxp3^+$ $CD25^+$ $CD95^+$ $CD4^+$ T cells, and defined as CXCR5 positive and CCR7 negative, consistent with GC location, and as CXCR5 negative and CCR7 positive, consistent with T-zone location, respectively (Figure 1B). Of note, the T_{REG} population identified by this strategy only includes a specific subset based on the expression or the lack thereof of the two considered chemokines. We will refer to this subset as $CCR7^+$-T_{REG} or T_{REG} for simplicity.

In agreement with Sage *et al.* and Linterman *et al.*, we used the Foxp3 marker to distinguish between T_{FH} and T_{FR} subsets because both populations express CXCR5, PD-1, ICOS and Bcl-6 (48)(25). T_{FH} were defined as $Foxp3^{neg}$ $CXCR5^+$ PD-1^{high} $CD4^+$ T cells (Figure 1B).

Consistent with their mouse counterparts, macaque T_{FR} expressed comparable levels of Foxp3 (Figure 1C), equal intensity and frequency of CD25, and frequency of CD39 to T_{REG} (Figure 1D and Supplemental Figure 1A and B) (25)(26). T_{FR} were also negative for CD127, the marker for the IL-7 receptor, and expressed common T_{FH} markers, such as PD-1, Bcl-6 and ICOS (Supplemental Figure 1C and Figure 1E) (28). Only a subset of T_{REG} but not of T_{FR} or T_{FH} cells was positive for the αE (CD103) and α4β7 integrin (25)(26) (Figure 1E and **data not shown**).

Within the $Foxp3^+$ $CD25^+$ population we identified an additional $CXCR5^+$ $CCR7^+$ double positive (DP) cell subset (Figure 1B). DP cells expressed intermediate levels of PD-1 as compared to T_{FR} and T_{REG} and had equal levels of Bcl-6 to T_{FR} cells (Supplemental Figure 1D).

We looked at the distribution of T_{FR}, T_{REG} and T_{FH} in blood, peripheral lymph nodes, and in the gut-associated lymphoid tissue (GALT; colon, jejunum and rectal mucosa) obtained from 6, 21 and 8 naïve macaques, respectively (Figure 1F–H). Representative flow plots obtained from blood, lymph node and rectal mucosa tissue from one healthy animal are shown in Supplemental Figure 1E. T_{FR} were mainly in the GALT and lymph nodes, and only a few were detected in blood (Figure 1F and Supplemental Figure 1E). Within the $Foxp3^+$ $CD25^+$ population, cells that expressed only CXCR5 were less frequent in lymph nodes than in the GALT ($p<0.0001$ by the Wilcoxon rank sum test; Figure 1F, upper panel), and the opposite was observed for cells that expressed only CCR7 ($p<0.0001$ by the Wilcoxon rank sum test; Figure 1G, upper panel). The apparent difference in tissue distribution in lymph nodes and GALT was lost when we looked at the frequency of T_{FR} and T_{REG} within the memory $CD4^+$ T cell population (lower panels Figure 1F and G). DP cells were equally distributed among all the tissues analyzed, including the blood (Supplemental Figure 1F). Finally T_{FH} frequency was significantly higher in lymph nodes and in the GALT than in the blood, as previously described (PBMCs vs. LN, $p<0.0001$; PBMCs vs. GALT, $p=0.0031$) (49) (Figure 1H).

Because we could not determine whether DP cells home exclusively to the B-zone, we excluded them from the rest of the analysis.

Macaque T_{FR} suppress $CD4^+$ T cells and T_{FH} proliferation of in vitro

In mice, T_{FR} control T_{FH} numbers and decrease their proliferation *in vivo* and *in vitro* (26). We studied if macaque's lymph nodes also contained a suppressive $CD4^+$ T cell population that homes to the B follicles. We sorted $CD4^+$ $CD25^+$ live cells from the lymph nodes of 2 naïve animals and isolated those capable of migrating in response to CXCL13, the ligand for CXCR5 (Figure 2). While we could not use Foxp3, an intracellular marker, to discriminate suppressor $CD4^+$ T cells, sorted $CD25^+$ $CD4^+$ T cells from lymph nodes consisted primarily of $Foxp3^+$ $CD4^+$ T cells (Figure 2A). Regulatory $CD4^+$ T cells that migrated to CXCL13 had higher levels of CXCR5, lower levels of CCR7 and expressed higher levels of Bcl-6 than those that did not migrate (Figure 2B). This strategy allowed us to obtain a population of $CD4^+$ T cells, highly enriched for T_{FR}, which could be used in downstream functional assays. Unsorted and sorted cells were stimulated with or without CD3 and CD28, in the presence or absence of migrated $CD25^+$ $CD4^+$ T cells (follicular-T_{REG}-enriched population). We assessed proliferation (% of $CFSE^{dim}$ cells) within $CXCR5^+$ $PD\text{-}1^{high}$ $CD4^+$ T cells (T_{FH} gated cells) by FACS analysis. Representative plots of the gated $CXCR5^+$ $CD4^+$ T cells (*Gate 1)* are shown in Supplemental Figure 2A. Interestingly, in both the two lymph nodes used for this analysis, T_{FH} proliferated less in the presence of T_{FR}-enriched cells following stimulation than in the absence of $CD25^+$ cells, as shown in the representative plots in Figure 2C and graphically in Figure 2D. As expected, T_{FR} also reduced non-T_{FH} $CD4^+$ T cells subsets proliferation (*Gate 2*), Supplemental Figure 2B).

Consistent with their regulatory function and similar to T_{REG}, T_{FR} produce IL-10 and TGF-β, which together suppress the proliferative potential and function of $CD4^+$ T cells in mice (50) (51). Thus, we measured the levels of IL-10 and TGF-β in enriched populations of T_{FR} ($CD3^+$ $CD4^+$ $CD25^+$ $CXCR5^+$ $CCR7^-$) and $CCR7^+$-T_{REG} ($CD3^+$ $CD4^+$ $CD25^+$ $CXCR5^-$ $CCR7^+$) obtained from peripheral lymph nodes of 3 naïve macaques. T_{FR} had equivalent IL-10 and TGF-β mRNA levels, by RT-PCR, than $CCR7^+$-T_{REG} (Figure 2E and F).

SIV_{mac251} infection and T_{FR} cell frequency

Sorted T_{FR} and T_{REG} from lymph nodes of 4 chronically infected macaques expressed comparable levels of CCR5 (Figure 3A), and harbored equivalent levels of SIV-DNA (Figure 3B). Similar SIV-DNA levels were also found in T_{FH} cells.

We analyzed the effect of SIV_{mac251} infection on the frequency of T_{FR} and $CCR7^+$-T_{REG} in the lymph nodes of 10 acutely (2 or 3 weeks after infection) and 23 chronically infected (12–15 weeks after infection) macaques (Figure 3C and D, Table I). Representative dot-plots for 2 macaques before and after infection are shown in Supplemental Figure 3A. Cells expressing only $CXCR5^+$ were significantly reduced within the $Foxp3^+$ $CD25^+$ population during chronic infection (chronic vs. negative $p< 0.0001$; chronic vs. acute $p< 0.0001$) (Figure 3C), while CCR7-single positive cells simultaneously increased (chronic vs. negative $p<0.0001$; chronic vs. acute $p= 0.0003$) when compared to non-infected and chronically infected animals (Figure 3D).

We looked at the levels of T_{FR} and $CCR7^+$-T_{REG} with respect to the memory $CD95^+$ $CD4^+$ T population. T_{FR} showed a downward trend from negative to acute to chronic ($p=0.0005$ by

the Jonckheere-Terpstra test for trend), with marginal differences in acute (negative vs. acute: p=0.049), and a significant decrease in chronic infection (negative vs. chronic p=0.0003) (Figure 3E). A trend for increase in $CCR7^+$-T_{REG} levels was also observed and significance was reached between the values detected in acute and in chronic phase (p=0.0018) (Figure 3F).

We then performed immunohistochemistry in lymph nodes, at 3 and 12 weeks after infection from 7 and 8 animals, respectively (Figure 3G and H). The numbers of $CD3^+$ cells expressing Foxp3 in the B-cell follicles was significantly reduced in acute infection (p=0.0022, n=7) and contracted even further in chronic infection (p<0.0001, n=8), when compared to naïve (n=8) animals (Figure 3G and Supplemental Figure 3B). The number of $Foxp3^+$ $CD3^+$ cells in the T-zone did not change, as described by others (Figure 3H) (52).

We did not see any significant correlation between the frequency of T_{FR} or T_{REG} and the SIV-RNA plasma levels (**data not shown**).

To further explore possible mechanisms for the SIV-associated decrease of T_{FR}, we looked at markers of immune activation. We could not find any association with the frequency of $Ki67^+$ $CD4^+$ T cells in lymph nodes of 10 chronic animals (**data not shown)**.

In mice NFAT-2 is critical for the up-regulation of CXCR5 on T_{FR} (31), hence for their migration to the GC. Thus NFAT-2 may be involved in the reduction of T_{FR} during chronic infection. To determine whether CXCR5 expression on macaque T_{FR} was also dependent on NFAT activity, we treated lymph nodes cells from 2 naïve animals with cyclosporin A (CsA), and measured changes in the CXCR5 and CCR7 levels within $Foxp3^+$ $CD25^+$ $CD4^+$ T cells (Supplemental Figure 3C and D). While CsA treatment had no effect on CCR7, it decreased CXCR5 expression levels on $Foxp3^+$ $CD25^+$ $CD4^+$ T cells.

Decreased T_{FR} and increased T_{FH} frequency during SIV_{mac251} infection

The decrease of $CXCR5^+$ regulatory T-cells may be associated with T_{FH} expansion during SIV_{mac251} infection. We measured the frequency of T_{FH} in lymph nodes of infected macaques as shown in Figure 1B. The percentage of T_{FH} cells within the memory $CD4^+$ T cell population did not change during acute infection but this population significantly expanded during chronic infection (week 12–15 after infection), as described by others (8) (negative vs. chronic and acute vs. chronic p<0.0001) (Figure 4A and B). Of note, we found a significant inverse correlation between the levels of T_{FR} and T_{FH} on memory $CD4^+$ T cells during acute and chronic infection (R=−0.82, p=0.0058 and R=−0.69, p= 0.0010 by the Spearman Rank test) (Figure 4B and 4C).

T_{FR} frequency correlates with decreased avidity of antibodies to the gp120

In mice, T_{FR} cells play a role in reducing plasma-cell differentiation (26). We measured the frequency of IgM^+, IgG^+ or IgA^+ $CD20^+$ B cells and plasmablasts, defined as $lineage^-$ ($CD3^-$ $CD14^-$ $CD16^-$ $CD56^-$) $CD20^+$ and/or $CD19^+$ and $CD21^-$ $Ki67^+$ $CD38^+$ $CD39^+$ in lymph nodes of SIV_{mac251} chronically infected animals (n=14) by flow cytometry. While we did not find any associations with the frequency of total memory B cells or plasmablasts measured in lymph nodes, we found a weak negative correlation between the frequency of

IgG$^+$ B cells and the frequency of IgM-switched plasmablasts (IgG$^+$ and IgA$^+$) and the percentage of T_{FR} within Foxp3$^+$ CD25$^+$ cells (Figure 5A and B).

T_{FH} are associated with the avidity to influenza virus and SIV (8)(53). In SIV_{mac251} infected macaques, avidity to the gp120 is low during acute infection and increases during chronic infection (Figure 5C). We confirmed that T_{FH} were positively associated with gp120 avidity when all the infected macaques were considered (R=0.88; p=0.0031; Figure 5D), but not when the acute and chronic phases values were looked at separately. Importantly, T_{FR} levels on memory CD4$^+$ T cells were associated with a reduction of binding high avidity antibodies to SIV-gp120 in all the infected animals (R=−0.85; p=0.0061, and in chronic phase (R=−1.0 and p=0.017), but not during the acute phase (R=−0.80; p=0.33) (Figure 5E and F and **data not shown**).

Discussion

In this study we identified T_{FR} in lymphoid tissues of healthy non-vaccinated rhesus macaques. We confirmed the presence of Foxp3$^+$ T cells in the B-zone of intact lymph nodes of macaques. Because T_{FR} share markers of T_{FH} and T_{REG}, they have been isolated and functionally characterized in mice as T_{FH} cells positive for Foxp3 (25), or alternatively, as “follicular” T_{REG} expressing CXCR5 (26)(47). We opted for the latter identification strategy to characterize macaque T_{FR} in lymph nodes. In addition, we identified a subset of CCR7-expressing T_{REG} that are CXCR5 negative and therefore, in principle, unable to enter the GC, and another subset of CXCR5 & CCR7-positive T_{REG} (DP). Because it is possible that DP may localize at the T-B borders/mantle zone, following gradients of CXCL13 (B-cell follicles-GC) and of CCL21 and CCL19 (T-zone), we excluded this population from our analysis (7).

In accordance with their mouse counterpart, macaque T_{FR} expressed high levels of PD-1, ICOS and Bcl-6, they were CD39$^+$ and CD127$^-$, and mainly resided in the GALT and lymph nodes. In a few macaques, T_{FR} had similar levels of IL-10 and TGF-β mRNA as CCR7$^+$-T_{REG} (25, 26). It is possible that IL-10 and TGF-β may play a role in the T_{FR}-mediated control of T_{FH} proliferation, as shown in mice. We did not directly assess the suppressive ability of sorted CD25$^+$ CXCR5$^+$ CCR7$^-$ cells, however lymph nodes of healthy non-infected macaques contained a CXCR5^{high} CCR7^{low} Bcl-6^{hi} CD25$^+$ CD4$^+$ population displaying *in vitro* chemotaxis toward CXCL13, and suppressive activity on CD4$^+$ T cells and T_{FH} proliferation. Further characterization is needed to confirm IL-10 and TGF-β production by macaque T_{FR} and their role in the apparent suppression.

We took advantage of the established similarities between SIV-infection of macaques and HIV-1 infection of humans to study and T_{FR} susceptibility and dynamic during infection in comparison to CCR7$^+$-$T_{REG.}$ Previous studies on CD4$^+$ T susceptibility have shown that CD25$^+$ Foxp3$^+$ cells are less susceptible than other subsets to HIV/SIV infection, due to their anergic nature and to the Foxp3-mediated inhibition of HIV-1-LTR activation (54)(55)(56)(57). Therefore the relative frequency of CD25$^+$ Foxp3$^+$ CD4$^+$ T increases in acute and chronic HIV/SIV infection, while their absolute number remains the same (58)(59)(56). Similarly, we observed a trend for increased frequency of CCR7$^+$-T_{REG} within the memory

$CD4^+$ population and no differences in the number of $CD3^+Foxp3^+$ cells in the T-zone of intact lymph nodes in chronic infection.

T_{FR} from naïve macaques expressed comparable levels of surface CCR5 to T_{REG}, and had equivalent levels of SIV-DNA following infection. Conversely, we saw a reduction in T_{FR} frequency and a decrease of $CD3^+$ $Foxp3^+$ cells in the B-follicles of infected animals, in particular during the chronic phase of infection. While we could not discern between $CD8^+$ T cells and $CD4^+$ T cells in our immunohistochemical analysis, some chronically infected animals had negligible numbers of $Foxp3^+$ T cells in the GC indicating an overall reduction of regulatory cells, likely including T_{FR}.

We could not determine whether T_{FR} are more susceptible to SIV_{mac251} infection than T_{REG}, and we did not observe any association between the T_{FR} levels and viral replication levels or with immune activation.

The reduction in $Foxp3^+$ cells in the GC may be driven by SIV-associated changes in the homing patterns of these cells. NFAT-2 is an essential transcriptional factor for CXCR5 expression on mice T_{FR} (31). HIV-envelope induces NFAT-2 translocation to the nucleus, where it binds to multiple sites within the HIV-LTR (60)(61). HIV/SIV may therefore alter NFAT-dependent expression of CXCR5. We showed that cyclosporin A, a calcineurin inhibitor that blocks NFAT dephosphorylation, decreases CXCR5 levels on macaque $CD4^+CD25^+Foxp3^+$ cells, but we were unable to test this intriguing hypothesis in our model due to the lack of reagents that cross-react with macaque NFAT proteins.

T_{FH} numbers expand in acute and chronic viral infections, such as in Influenza A virus (IAV) infection in mice, and in chronic Hepatitis B and HIV/SIV in humans and macaques (62)(63, 64). In particular during acute IAV infection, a temporary T_{FH} expansion occurs 3 days after challenge (62). Differently, in HIV/SIV infection, a sustained expansion of T_{FH} is seen in chronic, but not during the acute phase of infection, as we also observed in our study (8).

We found an association between the levels of T_{FR} and T_{FH} in acutely and chronic macaques infected with SIV_{mac251}. It is possible that a reduction or lack of expansion of T_{FR} may contribute to the increased T_{FH} number in chronic infection. Alternatively, the persistence of the antigen may lead to the increase in T_{FH} cells, resulting in higher levels of PD-1 in the GC and in T_{FR} reduction (47). Additionally, changes in T_{FR} function, other regulatory subsets in the GC ($CD8^+$ and NK T-cells), imbalanced cytokine milieu (i.e. increased IL-6), and immune activation are likely to participate to the HIV-associated increase in T_{FH} numbers (8)(19).

To our knowledge our study is the first to describe T_{FR} dynamics and changes in the T_{FH}/T_{FR} ratio during SIV infection, together with the accompanied study by Chowdhury and colleagues reporting similar findings in SIV_{smE660} infected macaques.

By suppressing T_{FH} numbers and proliferation, T_{FR} modulate B-cell responses in mice (26) (29)(47). No correlation was found with the frequency of plasmablasts or with the IgA^+ B cells. We found an association between the relative frequency of $CXCR5^+$ cells within the

$CD25^+$ $Foxp3^+$ population and the frequency of total IgG^+ B cells and of overall switched IgM^- (IgA^+ IgG^+) B-cells and plasmablasts in lymph nodes (32).

The accumulation of T_{FH} in chronic SIV infection is associated with increased titers of higher avidity SIV-specific immunoglobulins (8). Interestingly, we observed an antithetic role of T_{FR} and T_{FH} in the avidity of antibodies to the SIV-gp120 protein throughout the infection, and only T_{FR} levels were strongly correlated with the increased in avidity during chronic infection. It has been proposed that T_{FH} accumulation, together with HIV-associated changes in cell function, may lead to a reduction in affinity maturation due to a lowered competition for B-cell selection. However, so far, the role of T_{FH} cells in HIV/SIV pathogenesis has been studied without making a clear distinction between T_{FR} and T_{FH}. Thus, the relative contribution of T_{FH} and T_{FR} in the impairment in B-cell selection during HIV infection remains to be determined.

In summary, we identified a population of macaques $CD4^+$ T cells with a phenotype, function and location consistent with T_{FR} cells, and we revealed SIV-associated changes in the T_{FR} and T_{FH} ratio, adding to the complexity of humoral immunity to HIV.

Supplementary Material

Refer to Web version on PubMed Central for supplementary material.

Acknowledgments

We thank James Arthos and Claudia Cicala for helpful discussion, and Namal P. Liyanage and Dallas P. Brown and Veronica Galli for critical reading of the manuscript.

This work was entirely supported by the Intramural Research Program at the National Cancer Institute, National Institutes of Health.

Nonstandard abbreviations

$\mathbf{T_{REGS}}$	T regulatory cells
$\mathbf{T_{FH}}$	T follicular helper
$\mathbf{T_{FR}}$	T follicular regulatory cells

References

1. Garside P, Ingulli E, Merica RR, Johnson JG, Noelle RJ, Jenkins MK. Visualization of specific B and T lymphocyte interactions in the lymph node. Science. 1998; 281:96–99. [PubMed: 9651253]
2. Liu YJ, Zhang J, Lane PJ, Chan EY, MacLennan IC. Sites of specific B cell activation in primary and secondary responses to T cell-dependent and T cell-independent antigens. European journal of immunology. 1991; 21:2951–2962. [PubMed: 1748148]
3. Jacob J, Kelsoe G, Rajewsky K, Weiss U. Intraclonal generation of antibody mutants in germinal centres. Nature. 1991; 354:389–392. [PubMed: 1956400]
4. Schwickert TA, Victora GD, Fooksman DR, Kamphorst AO, Mugnier MR, Gitlin AD, Dustin ML, Nussenzweig MC. A dynamic T cell-limited checkpoint regulates affinity-dependent B cell entry into the germinal center. The Journal of experimental medicine. 2011; 208:1243–1252. [PubMed: 21576382]

5. Kim CH, Rott LS, Clark-Lewis I, Campbell DJ, Wu L, Butcher EC. Subspecialization of CXCR5+ T cells: B helper activity is focused in a germinal center-localized subset of CXCR5+ T cells. The Journal of experimental medicine. 2001; 193:1373–1381. [PubMed: 11413192]

6. Ansel KM, McHeyzer-Williams LJ, Ngo VN, McHeyzer-Williams MG, Cyster JG. In vivo-activated CD4 T cells upregulate CXC chemokine receptor 5 and reprogram their response to lymphoid chemokines. The Journal of experimental medicine. 1999; 190:1123–1134. [PubMed: 10523610]

7. Schaerli P, Willimann K, Lang AB, Lipp M, Loetscher P, Moser B. CXC chemokine receptor 5 expression defines follicular homing T cells with B cell helper function. The Journal of experimental medicine. 2000; 192:1553–1562. [PubMed: 11104798]

8. Petrovas C, Yamamoto T, Gerner MY, Boswell KL, Wloka K, Smith EC, Ambrozak DR, Sandler NG, Timmer KJ, Sun X, Pan L, Poholek A, Rao SS, Brenchley JM, Alam SM, Tomaras GD, Roederer M, Douek DC, Seder RA, Germain RN, Haddad EK, Koup RA. CD4 T follicular helper cell dynamics during SIV infection. The Journal of clinical investigation. 2012; 122:3281–3294. [PubMed: 22922258]

9. Hong JJ, Amancha PK, Rogers KA, Courtney CL, Havenar-Daughton C, Crotty S, Ansari AA, Villinger F. Early lymphoid responses and germinal center formation correlate with lower viral load set points and better prognosis of simian immunodeficiency virus infection. Journal of immunology. 2014; 193:797–806.

10. Breitfeld D, Ohl L, Kremmer E, Ellwart J, Sallusto F, Lipp M, Forster R. Follicular B helper T cells express CXC chemokine receptor 5, localize to B cell follicles, and support immunoglobulin production. The Journal of experimental medicine. 2000; 192:1545–1552. [PubMed: 11104797]

11. Crotty S. Follicular helper CD4 T cells (TFH). Annual review of immunology. 2011; 29:621–663.

12. Johnston RJ, Poholek AC, DiToro D, Yusuf I, Eto D, Barnett B, Dent AL, Craft J, Crotty S. Bcl6 and Blimp-1 are reciprocal and antagonistic regulators of T follicular helper cell differentiation. Science. 2009; 325:1006–1010. [PubMed: 19608860]

13. Nurieva RI, Chung Y, Martinez GJ, Yang XO, Tanaka S, Matskevitch TD, Wang YH, Dong C. Bcl6 mediates the development of T follicular helper cells. Science. 2009; 325:1001–1005. [PubMed: 19628815]

14. Chtanova T, Tangye SG, Newton R, Frank N, Hodge MR, Rolph MS, Mackay CR. T follicular helper cells express a distinctive transcriptional profile, reflecting their role as non-Th1/Th2 effector cells that provide help for B cells. Journal of immunology. 2004; 173:68–78.

15. Vinuesa CG, Linterman MA, Goodnow CC, Randall KL. T cells and follicular dendritic cells in germinal center B-cell formation and selection. Immunological reviews. 2010; 237:72–89. [PubMed: 20727030]

16. Schmitt N, Bustamante J, Bourdery L, Bentebibel SE, Boisson-Dupuis S, Hamlin F, Tran MV, Blankenship D, Pascual V, Savino DA, Banchereau J, Casanova JL, Ueno H. IL-12 receptor beta1 deficiency alters in vivo T follicular helper cell response in humans. Blood. 2013; 121:3375–3385. [PubMed: 23476048]

17. Vinuesa CG, Sanz I, Cook MC. Dysregulation of germinal centres in autoimmune disease. Nature reviews Immunology. 2009; 9:845–857.

18. Goodnow CC, Vinuesa CG, Randall KL, Mackay F, Brink R. Control systems and decision making for antibody production. Nature immunology. 2010; 11:681–688. [PubMed: 20644574]

19. Pratama A, Vinuesa CG. Control of TFH cell numbers: why and how? Immunology and cell biology. 2014; 92:40–48. [PubMed: 24189162]

20. de Vinuesa CG, Cook MC, Ball J, Drew M, Sunners Y, Cascalho M, Wabl M, Klaus GG, MacLennan IC. Germinal centers without T cells. The Journal of experimental medicine. 2000; 191:485–494. [PubMed: 10662794]

21. Warnatz K, Bossaller L, Salzer U, Skrabl-Baumgartner A, Schwinger W, van der Burg M, van Dongen JJ, Orlowska-Volk M, Knoth R, Durandy A, Draeger R, Schlesier M, Peter HH, Grimbacher B. Human ICOS deficiency abrogates the germinal center reaction and provides a monogenic model for common variable immunodeficiency. Blood. 2006; 107:3045–3052. [PubMed: 16384931]

22. King C, Tangye SG, Mackay CR. T follicular helper (TFH) cells in normal and dysregulated immune responses. Annual review of immunology. 2008; 26:741–766.
23. Park HJ, Kim DH, Lim SH, Kim WJ, Youn J, Choi YS, Choi JM. Insights into the role of follicular helper T cells in autoimmunity. Immune network. 2014; 14:21–29. [PubMed: 24605077]
24. Linterman MA, Rigby RJ, Wong RK, Yu D, Brink R, Cannons JL, Schwartzberg PL, Cook MC, Walters GD, Vinuesa CG. Follicular helper T cells are required for systemic autoimmunity. The Journal of experimental medicine. 2009; 206:561–576. [PubMed: 19221396]
25. Linterman MA, Pierson W, Lee SK, Kallies A, Kawamoto S, Rayner TF, Srivastava M, Divekar DP, Beaton L, Hogan JJ, Fagarasan S, Liston A, Smith KG, Vinuesa CG. Foxp3+ follicular regulatory T cells control the germinal center response. Nature medicine. 2011; 17:975–982.
26. Chung Y, Tanaka S, Chu F, Nurieva RI, Martinez GJ, Rawal S, Wang YH, Lim H, Reynolds JM, Zhou XH, Fan HM, Liu ZM, Neelapu SS, Dong C. Follicular regulatory T cells expressing Foxp3 and Bcl-6 suppress germinal center reactions. Nature medicine. 2011; 17:983–988.
27. Lim HW, Hillsamer P, Banham AH, Kim CH. Cutting edge: direct suppression of B cells by CD4+ CD25+ regulatory T cells. Journal of immunology. 2005; 175:4180–4183.
28. Lim HW, Hillsamer P, Kim CH. Regulatory T cells can migrate to follicles upon T cell activation and suppress GC-Th cells and GC-Th cell-driven B cell responses. The Journal of clinical investigation. 2004; 114:1640–1649. [PubMed: 15578096]
29. Alexander CM, Tygrett LT, Boyden AW, Wolniak KL, Legge KL, Waldschmidt TJ. T regulatory cells participate in the control of germinal centre reactions. Immunology. 2011; 133:452–468. [PubMed: 21635248]
30. Oestreich KJ, Mohn SE, Weinmann AS. Molecular mechanisms that control the expression and activity of Bcl-6 in TH1 cells to regulate flexibility with a TFH-like gene profile. Nature immunology. 2012; 13:405–411. [PubMed: 22406686]
31. Vaeth M, Muller G, Stauss D, Dietz L, Klein-Hessling S, Serfling E, Lipp M, Berberich I, Berberich-Siebelt F. Follicular regulatory T cells control humoral autoimmunity via NFAT2-regulated CXCR5 expression. The Journal of experimental medicine. 2014; 211:545–561. [PubMed: 24590764]
32. Wolniak KL, Shinall SM, Waldschmidt TJ. The germinal center response. Critical reviews in immunology. 2004; 24:39–65. [PubMed: 14995913]
33. Mqadmi A, Zheng X, Yazdanbakhsh K. CD4+CD25+ regulatory T cells control induction of autoimmune hemolytic anemia. Blood. 2005; 105:3746–3748. [PubMed: 15637139]
34. Moir S, Malaspina A, Ogwaro KM, Donoghue ET, Hallahan CW, Ehler LA, Liu S, Adelsberger J, Lapointe R, Hwu P, Baseler M, Orenstein JM, Chun TW, Mican JA, Fauci AS. HIV-1 induces phenotypic and functional perturbations of B cells in chronically infected individuals. Proceedings of the National Academy of Sciences of the United States of America. 2001; 98:10362–10367. [PubMed: 11504927]
35. De Milito A, Nilsson A, Titanji K, Thorstensson R, Reizenstein E, Narita M, Grutzmeier S, Sonnerborg A, Chiodi F. Mechanisms of hypergammaglobulinemia and impaired antigen-specific humoral immunity in HIV-1 infection. Blood. 2004; 103:2180–2186. [PubMed: 14604962]
36. Lindqvist M, van Lunzen J, Soghoian DZ, Kuhl BD, Ranasinghe S, Kranias G, Flanders MD, Cutler S, Yudanin N, Muller MI, Davis I, Farber D, Hartjen P, Haag F, Alter G, Schulze zur Wiesch J, Streeck H. Expansion of HIV-specific T follicular helper cells in chronic HIV infection. The Journal of clinical investigation. 2012; 122:3271–3280. [PubMed: 22922259]
37. Cubas RA, Mudd JC, Savoye AL, Perreau M, van Grevenynghe J, Metcalf T, Connick E, Meditz A, Freeman GJ, Abesada-Terk G Jr, Jacobson JM, Brooks AD, Crotty S, Estes JD, Pantaleo G, Lederman MM, Haddad EK. Inadequate T follicular cell help impairs B cell immunity during HIV infection. Nature medicine. 2013; 19:494–499.
38. Hong JJ, Amancha PK, Rogers K, Ansari AA, Villinger F. Spatial alterations between CD4(+) T follicular helper, B, and CD8(+) T cells during simian immunodeficiency virus infection: T/B cell homeostasis, activation, and potential mechanism for viral escape. Journal of immunology. 2012; 188:3247–3256.
39. Locci M, Havenar-Daughton C, Landais E, Wu J, Kroenke MA, Arlehamn CL, Su LF, Cubas R, Davis MM, Sette A, Haddad EK, Poignard P, Crotty S. A. V. I. P. C. P. I. International. Human

circulating PD-1+CXCR3-CXCR5+ memory Tfh cells are highly functional and correlate with broadly neutralizing HIV antibody responses. Immunity. 2013; 39:758–769. [PubMed: 24035365]

40. Vaccari M, Keele BF, Bosinger SE, Doster MN, Ma ZM, Pollara J, Hryniewicz A, Ferrari G, Guan Y, Forthal DN, Venzon D, Fenizia C, Morgan T, Montefiori D, Lifson JD, Miller CJ, Silvestri G, Rosati M, Felber BK, Pavlakis GN, Tartaglia J, Franchini G. Protection afforded by an HIV vaccine candidate in macaques depends on the dose of SIVmac251 at challenge exposure. Journal of virology. 2013; 87:3538–3548. [PubMed: 23325681]
41. Pegu P, Vaccari M, Gordon S, Keele BF, Doster M, Guan Y, Ferrari G, Pal R, Ferrari MG, Whitney S, Hudacik L, Billings E, Rao M, Montefiori D, Tomaras G, Alam SM, Fenizia C, Lifson JD, Stablein D, Tartaglia J, Michael N, Kim J, Venzon D, Franchini G. Antibodies with high avidity to the gp120 envelope protein in protection from simian immunodeficiency virus SIV(mac251) acquisition in an immunization regimen that mimics the RV-144 Thai trial. Journal of virology. 2013; 87:1708–1719. [PubMed: 23175374]
42. Cecchinato V, Tryniszewska E, Ma ZM, Vaccari M, Boasso A, Tsai WP, Petrovas C, Fuchs D, Heraud JM, Venzon D, Shearer GM, Koup RA, Lowy I, Miller CJ, Franchini G. Immune activation driven by CTLA-4 blockade augments viral replication at mucosal sites in simian immunodeficiency virus infection. Journal of immunology. 2008; 180:5439–5447.
43. De Vos J, Hose D, Reme T, Tarte K, Moreaux J, Mahtouk K, Jourdan M, Goldschmidt H, Rossi JF, Cremer FW, Klein B. Microarray-based understanding of normal and malignant plasma cells. Immunological reviews. 2006; 210:86–104. [PubMed: 16623766]
44. Vaccari M, Boasso A, Ma ZM, Cecchinato V, Venzon D, Doster MN, Tsai WP, Shearer GM, Fuchs D, Felber BK, Pavlakis GN, Miller CJ, Franchini G. CD4+ T-cell loss and delayed expression of modulators of immune responses at mucosal sites of vaccinated macaques following SIV(mac251) infection. Mucosal immunology. 2008; 1:497–507. [PubMed: 19079217]
45. Hofmann-Lehmann R, Swenerton RK, Liska V, Leutenegger CM, Lutz H, McClure HM, Ruprecht RM. Sensitive and robust one-tube real-time reverse transcriptase-polymerase chain reaction to quantify SIV RNA load: comparison of one-versus two-enzyme systems. AIDS research and human retroviruses. 2000; 16:1247–1257. [PubMed: 10957722]
46. Romano JW, Williams KG, Shurtliff RN, Ginocchio C, Kaplan M. NASBA technology: isothermal RNA amplification in qualitative and quantitative diagnostics. Immunological investigations. 1997; 26:15–28. [PubMed: 9037609]
47. Wollenberg I, Agua-Doce A, Hernandez A, Almeida C, Oliveira VG, Faro J, Graca L. Regulation of the germinal center reaction by Foxp3+ follicular regulatory T cells. Journal of immunology. 2011; 187:4553–4560.
48. Sage PT, Francisco LM, Carman CV, Sharpe AH. The receptor PD-1 controls follicular regulatory T cells in the lymph nodes and blood. Nature immunology. 2013; 14:152–161. [PubMed: 23242415]
49. Xu H, Wang X, Lackner AA, Veazey RS. PD-1(HIGH) Follicular CD4 T Helper Cell Subsets Residing in Lymph Node Germinal Centers Correlate with B Cell Maturation and IgG Production in Rhesus Macaques. Frontiers in immunology. 2014; 5:85. [PubMed: 24678309]
50. Li MO, Flavell RA. TGF-beta: a master of all T cell trades. Cell. 2008; 134:392–404. [PubMed: 18692464]
51. Sanjabi S, Zenewicz LA, Kamanaka M, Flavell RA. Anti-inflammatory and pro-inflammatory roles of TGF-beta, IL-10, and IL-22 in immunity and autoimmunity. Current opinion in pharmacology. 2009; 9:447–453. [PubMed: 19481975]
52. Arce J, Levin M, Xie Q, Albanese J, Ratech H. T-regulatory cells in lymph nodes: correlation with sex and HIV status. American journal of clinical pathology. 2011; 136:35–42. [PubMed: 21685030]
53. Leon B, Bradley JE, Lund FE, Randall TD, Ballesteros-Tato A. FoxP3+ regulatory T cells promote influenza-specific Tfh responses by controlling IL-2 availability. Nature communications. 2014; 5:3495.
54. Moreno-Fernandez ME, Zapata W, Blackard JT, Franchini G, Chougnet CA. Human regulatory T cells are targets for human immunodeficiency Virus (HIV) infection, and their susceptibility differs depending on the HIV type 1 strain. Journal of virology. 2009; 83:12925–12933. [PubMed: 19828616]

55. Li S, Gowans EJ, Chougnet C, Plebanski M, Dittmer U. Natural regulatory T cells and persistent viral infection. Journal of virology. 2008; 82:21–30. [PubMed: 17855537]

56. Tran TA, de Goer de Herve MG, Hendel-Chavez H, Dembele B, Le Nevot E, Abbed K, Pallier C, Goujard C, Gasnault J, Delfraissy JF, Balazuc AM, Taoufik Y. Resting regulatory CD4 T cells: a site of HIV persistence in patients on long-term effective antiretroviral therapy. PloS one. 2008; 3:e3305. [PubMed: 18827929]

57. Grant C, Oh U, Fugo K, Takenouchi N, Griffith C, Yao K, Newhook TE, Ratner L, Jacobson S. Foxp3 represses retroviral transcription by targeting both NF-kappaB and CREB pathways. PLoS pathogens. 2006; 2:e33. [PubMed: 16652169]

58. Chevalier MF, Weiss L. The split personality of regulatory T cells in HIV infection. Blood. 2013; 121:29–37. [PubMed: 23043072]

59. Boasso A, Vaccari M, Hryniewicz A, Fuchs D, Nacsa J, Cecchinato V, Andersson J, Franchini G, Shearer GM, Chougnet C. Regulatory T-cell markers, indoleamine 2,3-dioxygenase, and virus levels in spleen and gut during progressive simian immunodeficiency virus infection. Journal of virology. 2007; 81:11593–11603. [PubMed: 17715231]

60. Cicala C, Arthos J, Censoplano N, Cruz C, Chung E, Martinelli E, Lempicki RA, Natarajan V, VanRyk D, Daucher M, Fauci AS. HIV-1 gp120 induces NFAT nuclear translocation in resting CD4+ T-cells. Virology. 2006; 345:105–114. [PubMed: 16260021]

61. Rao A, Luo C, Hogan PG. Transcription factors of the NFAT family: regulation and function. Annual review of immunology. 1997; 15:707–747.

62. Boyden AW, Legge KL, Waldschmidt TJ. Pulmonary infection with influenza A virus induces site-specific germinal center and T follicular helper cell responses. PloS one. 2012; 7:e40733. [PubMed: 22792401]

63. Hu TT, Song XF, Lei Y, Hu HD, Ren H, Hu P. Expansion of circulating TFH cells and their associated molecules: involvement in the immune landscape in patients with chronic HBV infection. Virology journal. 2014; 11:54. [PubMed: 24655429]

64. Feng J, Lu L, Hua C, Qin L, Zhao P, Wang J, Wang Y, Li W, Shi X, Jiang Y. High frequency of CD4+ CXCR5+ TFH cells in patients with immune-active chronic hepatitis B. PloS one. 2011; 6:e21698. [PubMed: 21750724]

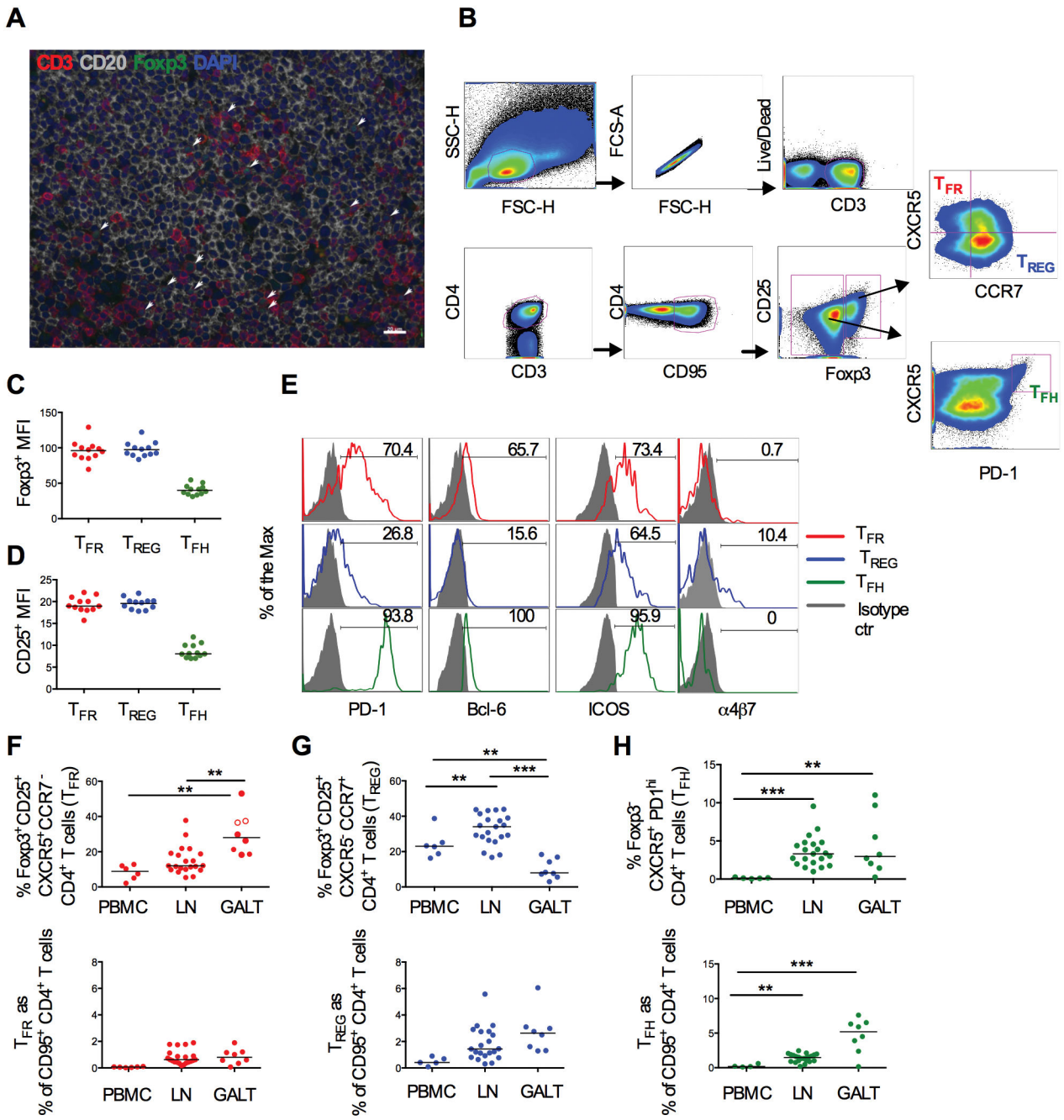

Figure 1. Characterization and distribution of T_{FR} in SIV-uninfected macaques

(A) Double positive $CD3^+$ (red) and $Foxp3^+$ cells (green) are present in B-follicles (CD20 in grey) in lymph nodes from a naïve macaque (blue =DAPI; scale bar: 20μm). **(B)** Representative flow cytometry plots showing the gating strategy for T_{FR}, $CCR7^+$-T_{REG} and T_{FH} cells in lymph nodes. All the subsets were gated on singlet/live/$CD3^+$ $CD4^+$ $CD95^+$. T_{FR} and $CCR7^+$-T_{REG} were identified as $Foxp3^+$ $CD25^+$ and $CXCR5^+$ $CCR7^-$ or $CXCR5^-$ $CCR7^+$, respectively; T_{FH} cells as $Foxp3^-$ $CXCR5^+$ $PD\text{-}1^{high}$. **(C)** Geometric mean (MFI) of Foxp3 and (**D**) CD25 expression. **(E)** Cell surface expression of PD-1, Bcl-6 ICOS and α4β7

in T_{FR} (red), T_{REG} (blue) and T_{FH} cells (green). Isotype controls are in grey. Frequency of **(F)** $CXCR5^+$ & $CCR7^-$ cells and **(G)** $CXCR5^-$ & $CCR7^+$ cells within $Foxp3^+$ $CD25^+$ $CD4^+$ T (upper panel) or within memory $CD4^+$ T cells (corresponding lower panels) in blood, peripheral lymph nodes and in the GALT (colon, jejunum and rectal mucosa) of naïve animals. The median is shown. (**H**) T_{FH} frequency on Foxp3 negative (upper panel) and memory $CD4^+$ T cells (lower panel) in different tissues.

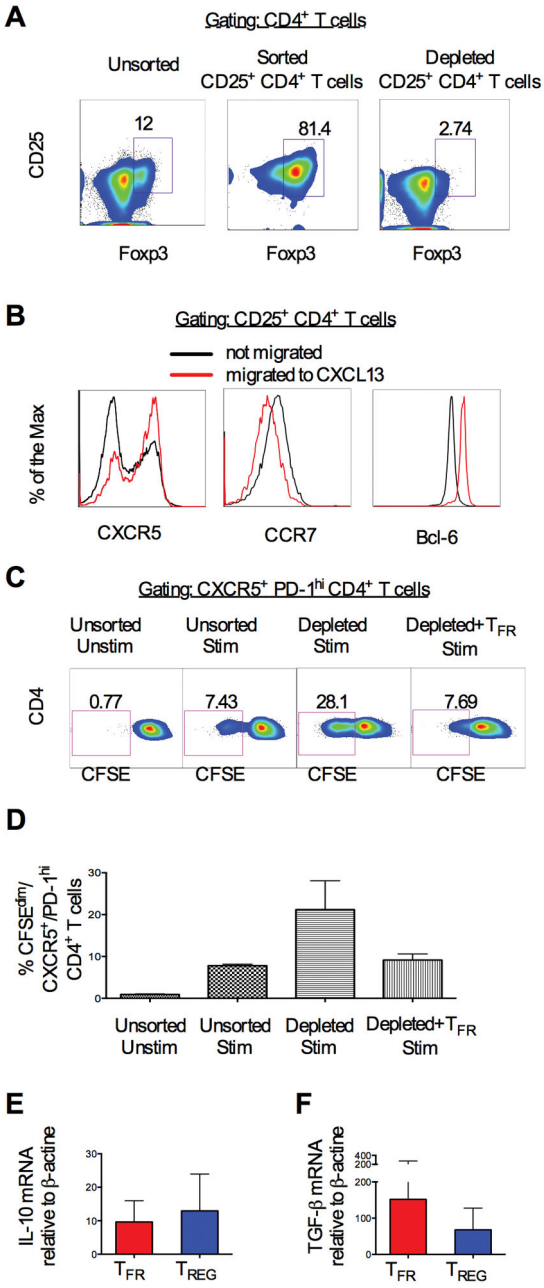

Figure 2. T_{FR} suppress *in vitro* T_{FH} cell proliferation

(**A**) Representative density plot showing unsorted (upper panel), sorted $CD25^+$ $CD4^+$ T cells (central panel) and $CD25^+$ $CD4^+$ T-depleted cells (lower panel) from a lymph node of a naïve macaque. **(B)** Cell surface expression of CXCR5, CCR7 and Bcl-6 on $CD4^+$ T cells that migrated (red line) or did not migrate (black line) to CXCL13. (**C**) Representative density plot showing proliferation ($CFSE^{dim}$) of stimulated (CD3, CD28) unsorted, $CD25^+$ depleted $CD4^+$ T cells alone or co-cultured with CXCL13 migrated-$CD25^+$ $CD4^+$ T cells. (**D**) Percentage of proliferating $CXCR5^+$ $PD1^{high}$ $CD4^+$ T cells in all conditions. The bars represent the mean ± standard error from 3 lymph nodes. (**E**) *IL-10* and (**F**) *TGF-β* mRNA

measured by RT-PCR from T_{FR} and $CCR7^{+}$-T_{REG} sorted from lymph nodes of 4 naïve animals. The bars represent the mean ± standard error.

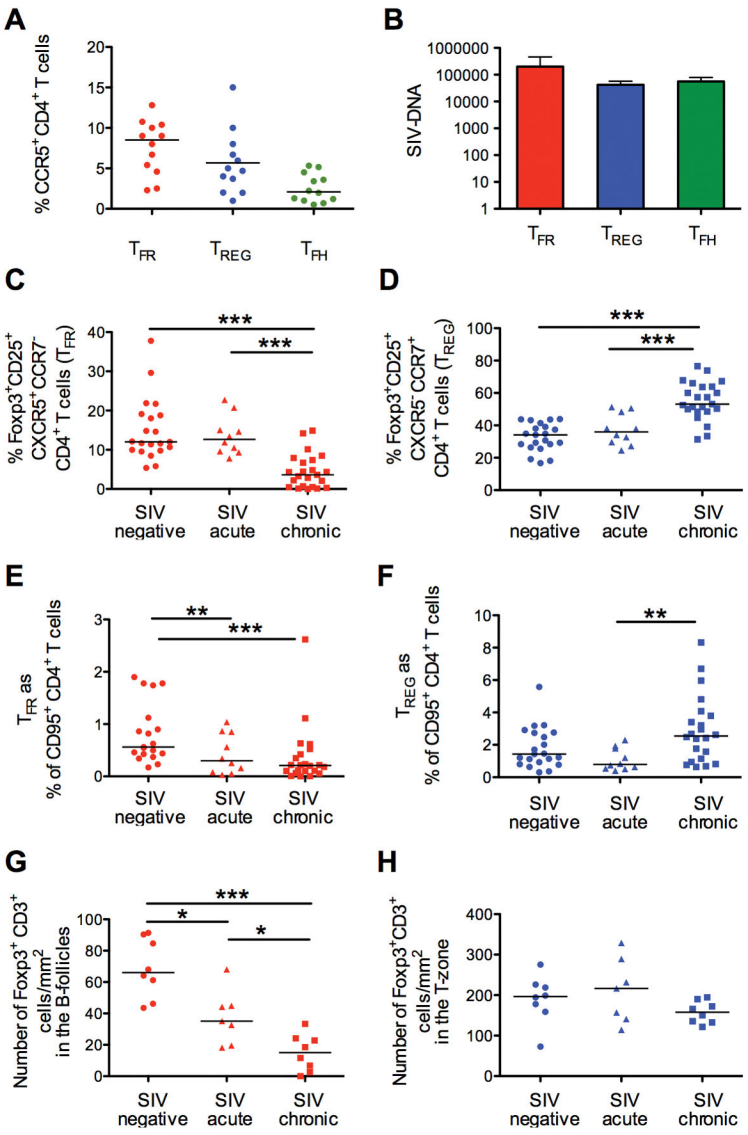

Figure 3. T_{FR} susceptibility and dynamics during SIV chronic infection

(A) Percentage of $CCR5^+$ T_{FR}, $CCR7^+$-T_{REG} and T_{FH}. **(B)** SIV-DNA levels in sorted T_{FR} $CCR7^+$-T_{REG} and T_{FH} by PCR. (**C)** Frequency of T_{FR} and **(D)** $CCR7^+$-T_{REG} within $Foxp3^+$ $CD25^+$ cells, and (**E**) T_{FR} and **(F)** $CCR7^+$-T_{REG} within memory $CD4^+$ T cells in lymph nodes of naïve, acutely and chronically SIV infected macaques. (**G)** Number of $Foxp3^+$ $CD3^+$ cells in the B-follicles (T_{FR}) and (**H**) in the T-zone (T_{REG}) of intact lymph nodes from naïve, acutely and chronically infected macaques.

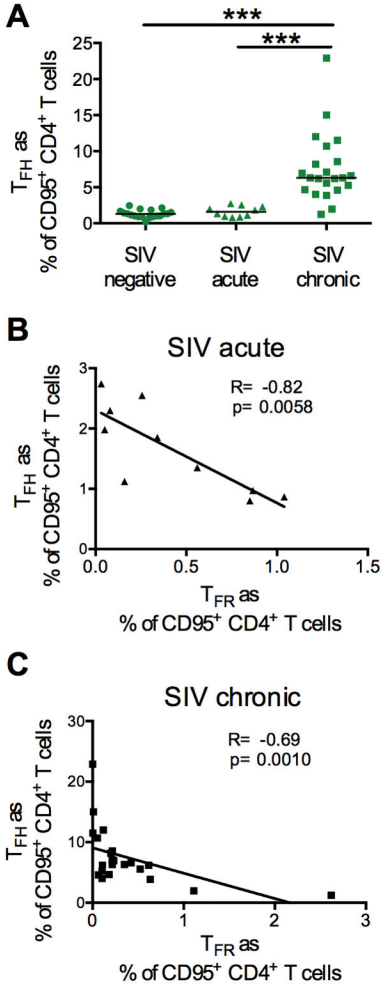

Figure 4. Association between T_{FR} and T_{FH} levels in SIV infection

(**A**) Frequency of T_{FH} on memory $CD4^+$ T cells in lymph nodes of naïve, acutely and chronic SIV-infected macaques. (**B**) Correlation between the percentage of T_{FR} and T_{FH} on memory $CD4^+$ T cells in acute and **(C)** chronic infection.

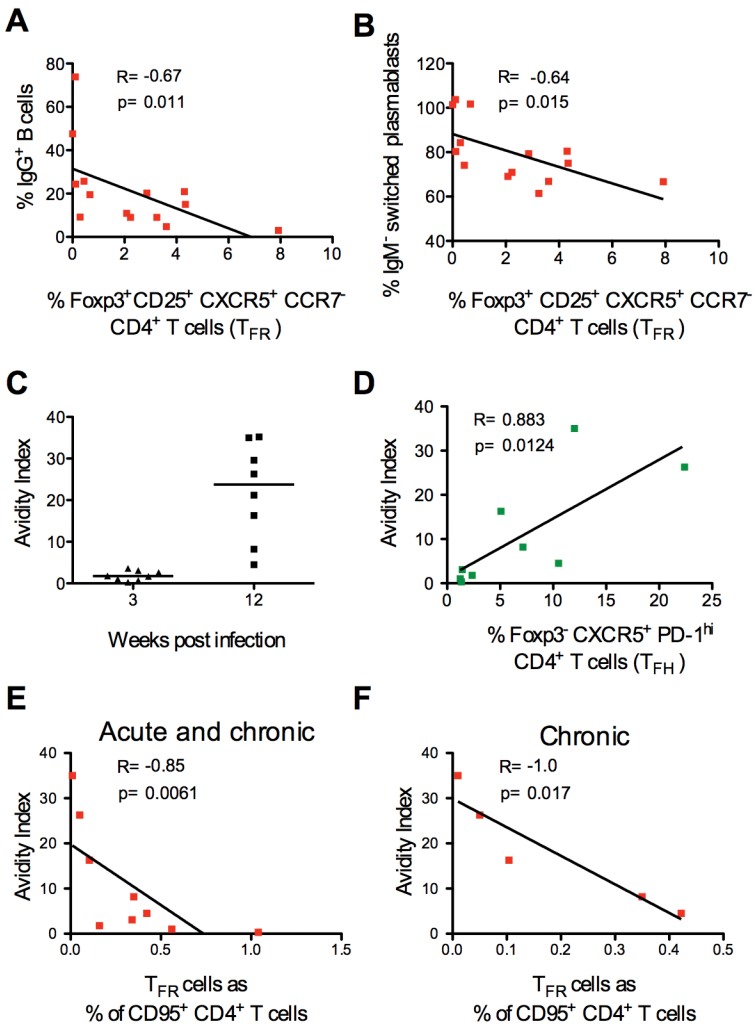

Figure 5. T_{FR} levels and SIV specific antibody avidity

(**A**) Correlation between the frequency of T_{FR} cells on $Foxp3^+$ $CD25^+$ cells and IgG^+ B cells or **(B)** switched IgM^- plasmablasts in lymph nodes of chronically infected macaques. (**C**) Avidity index of plasma SIV-gp120 IgG measured in acutely and chronically infected macaques (the median is shown). (**D**) Correlation between the frequency of T_{FH} or (**E**) T_{FR} cells and the avidity index in plasma of all the SIV infected macaques and (**F**) in chronically infected macaques.

Table I

Serological data, Acute and Chronic animals

Acute	Challenge	Weeks p.i	VL	CD4 count
P061	High dose I.R	2	5806601	748
P066	High dose I.R	2	25556960	489
P074	High dose I.R	2	30925780	333
P136	High dose I.R	2	39844500	382
P273	High dose I.R	2	34856014	524
P251	Low dose I.R	3	115008398	647
P434	Low dose I.R	3	215693077	517
P650	Low dose I.R	3	23469446	489
P716	Low dose I.R	3	108209623	454
P712	Low dose I.R	3	49568224	757

Chronic	Challenge	Weeks p.i	VL	CD4 count
P015	High dose I.R	14	121368	485
P061	High dose I.R	14	368663	928
P074	High dose I.R	14	11883300	437
P134	High dose I.R	14	16963740	260
P136	High dose I.R	14	19165270	340
P266	High dose I.R	15	172649	265
P273	High dose I.R	15	163587	360
P274	High dose I.R	15	1297398	265
E060	Low dose I.R	14	4957329	nd
E074	Low dose I.R	14	nd	nd
P632	Low dose I.R	12	7825190	111
P761	Low dose I.R	15	31347	1330
P758	Low dose I.R	15	24934	1431
P760	Low dose I.R	15	1425169	426
R158	Low dose I.R	15	1440103	820
P733	Low dose I.R	15	1358565	212
P746	Low dose I.R	15	143386	618
P754	Low dose I.R	15	2168071	734
P698	Low dose I.R	15	21182252	572
P609	Low dose I.R	15	5462462	239
P251	Low dose I.R	15	111656	406
P633	Low dose I.R	15	1104050	514
P761	Low dose I.R	15	147114	1330

Viral load: SIV/RNA copies/ml plasma Absolute $CD4^+$ T number/mm2 of blood

I.R= intrarectal; p.i. post infection; VL= viral load